Journal of Power Sources 251 (2014) 170–177

Contents lists available at ScienceDirect

Journal of Power Sources

journal homepage: www.elsevier.com/locate/jpowsour

Different failure modes for V-containing and V-free AB_2 metal hydride alloys

K. Young [a,*], D.F. Wong [a,b], S. Yasuoka [c], J. Ishida [c], J. Nei [a], J. Koch [a]

[a] BASF Battery Materials-Ovonic, 2983 Waterview Drive, Rochester Hills, MI 48309, USA
[b] Department of Chemical Engineering and Materials Science, Wayne State University, MI 48202, USA
[c] FDK Twicell Co., Ltd. 307-2 Koyagimachi, Takasaki 370-0071, Gunma, Japan

HIGHLIGHTS

- The capacity loss in V-containing AB_2 alloy is first slow and then faster.
- The capacity in the V-free AB_2 shows a consistent degradation.
- Failure mode of former is the formation of thick oxide on the surface.
- Failure mode of later is the continuous pulverization of the particles.

ARTICLE INFO

Article history:
Received 8 October 2013
Received in revised form
14 November 2013
Accepted 16 November 2013
Available online 27 November 2013

Keywords:
Hydrogen absorbing materials
Transition metal alloys
Metal hydride electrode
Electrochemical reactions

ABSTRACT

Failure modes of a V-containing and a V-free AB_2 Laves phase-based metal hydride alloy were studied by the combination of X-ray diffractometer, scanning electron microscope, X-ray energy dispersive spectroscopy, inductively coupled plasma, Soxhlet extraction, and magnetic susceptibility measurement. Cells with the V-containing alloy exhibited less capacity degradation up until venting occurred in the cells, after which the capacity rapidly degraded. Cells with the V-free alloy remained linear in capacity degradation throughout the cycle life test. The failure mechanism for the V-containing alloy is related to the formation of an oxide layer that penetrates deeper into the alloy particles due to high V leaching and impedes gas recombination, while the failure mechanism for the V-free alloy is related to the continuous pulverization of the main AB_2 phase.

1. Introduction

Nickel/metal hydride (Ni/MH) rechargeable batteries are widely used in consumer portable devices and hybrid electric vehicles, and development for these applications has a heavy emphasis on improving gravimetric energy density. While the conventional misch metal-based AB_5 metal hydride (MH) alloy has a storage capacity of about 330 mAh g^{-1}, AB_2 [1,2] and A_2B_7 [3] MH alloys have capacities as high as 440 and 410 mAh g^{-1}, respectively, and will boost the gravimetric energy density found in Ni/MH batteries. Properties relating to the structure, hydrogen storage, and electrochemistry of these new alloys have been reported extensively (for a review of research activities in these areas, see Ref. [4]); however, not much work has been reported regarding the failure mode analysis of these new alloys – an essential step of any new material development process. In a recent report, we compared the failure mode of La-only A_2B_7 alloy in a 70% state-of-charge cycling scheme to that of conventional AB_5 [5]. While the La-only A_2B_7 cell suffers from alloy pulverization, the AB_5 cell degrades due to alloy oxidation and consequent poisoning of the positive electrode.

V is an important modifying element used in AB_2 MH alloys to increase the storage capacity [6–11], facilitate activation [8], and improve both high-rate dischargeability [12] and cycle stability [13] in the Ni/MH negative electrode. However, the cost of V is much higher than other elements used in the typical AB_2 MH alloy formula. Studies optimizing composition [14] and modifier selection [15] were performed previously on V-free AB_2 MH alloys to reduce the raw material cost. In this paper, we will compare the failure modes of two Laves phase-based AB_2 MH alloys: one with V and one that is V-free that came out of the studies.

* Corresponding author. Tel.: +1 248 293 7000; fax: +1 248 299 4520.
E-mail addresses: kwoyoung@yahoo.com, kwo.young@basf.com (K. Young).

0378-7753/$ – see front matter © 2013 Elsevier B.V. All rights reserved.
http://dx.doi.org/10.1016/j.jpowsour.2013.11.035

Table 1
Structure, gaseous phase, electrochemical, and magnetic susceptibility properties comparison of Alloys A and B.

	Composition	Phase abundances	H-storage (wt.%)	Mid-point pressure (MPa)	PCT hysteresis	Cap. @ 50 mA g^{-1} (mAh g^{-1})	Cap. @ 5 mA g^{-1} (mAh g^{-1})	HRD	M_S (memu g^{-1})	$H_{1/2}$ (kOe)
Alloy A	$Ti_{12}Zr_{21.5}V_{10}Ni_{37.7}Mn_{13.5}Cr_{4.5}Al_{0.5}Sn_{0.3}$	78% C14, 20% C15, 1% Zr_7Ni_{10}, 1% Zr_9Ni_{11}	1.51	0.04	0.02	388	398	0.97	39	0.14
Alloy B	$Ti_{10}Zr_{27}Ni_{35}Co_5Mn_{15}Cr_8Al_{0.1}$	38% C14, 52% C15, 2.3% Zr_7Ni_{10}, 0.5% Zr_9Ni_{11}, 7% TiNi	1.61	0.12	0.42	341	374	0.91	27	0.60

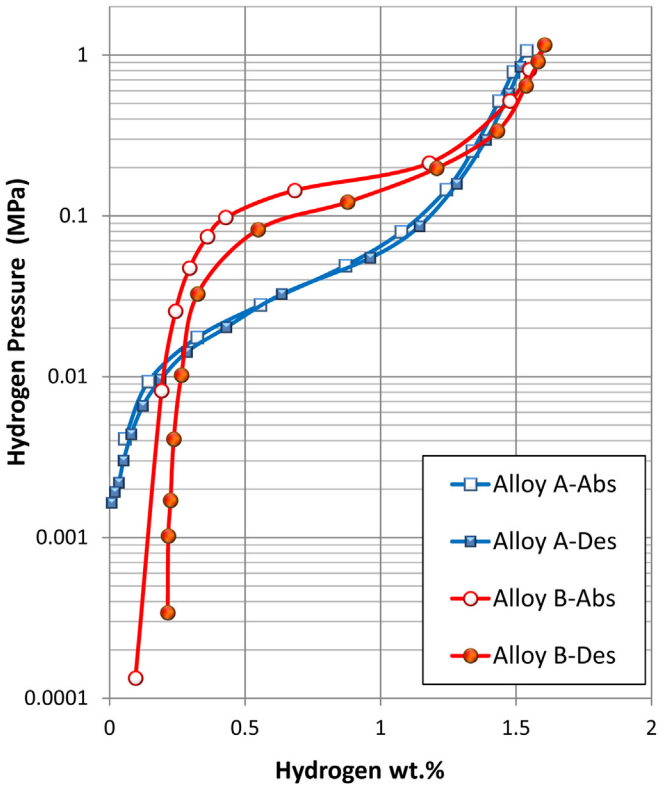

Fig. 1. PCT isotherms of Alloys A and B measured at 30 °C. Open and solid symbols are for absorption and desorption curves, respectively. The V-free alloy (Alloy B) shows a higher maximum storage capacity, a lower reversible storage capacity, a higher and flatter plateau, and a higher hysteresis.

2. Experimental setup

Induction melting from elementary raw materials was performed under an argon atmosphere in a 25 kg induction melting furnace using an MgO crucible, an alumina tundish, and a steel cylindrical mold. Ingots were first hydrided/dehydrided and then mechanically crushed into −200 mesh powder. The chemical composition of each sample was examined by a Varian *Liberty* 100 inductively-coupled plasma (ICP) system. A Philips *X'Pert Pro* X-ray diffractometer (XRD) was used to study the microstructure, and a JEOL-*JSM6320F* scanning electron microscope (SEM) with energy dispersive spectroscopy (EDS) capability was used to study the phase distribution and composition. Pressure–concentration–temperature (PCT) characteristics for each sample were measured using a Suzuki-Shokan multi-channel PCT system. Half-cell testing was performed using an Arbin Instruments BT4+ Portable Battery Test System. Magnetic susceptibility was measured using a Digital Measurement Systems Model 880 vibrating sample magnetometer. For full-cell testing, alloy powder was mixed with binder, pasted onto perforated Ni-plated stainless steel plate, dried, and compacted into negative electrodes. AA-sized cylindrical cells were assembled with pasted negative electrode, pasted $Ni(OH)_2$-based positive electrode, polypropylene/polyethylene grafted separator, and 30% KOH electrolyte. The cell design is targeted at a negative-to-positive ratio of 1.4 with a capacity of 1800 mAh. The MH alloy loading is around 7.2 g per cell.

3. Results and discussion

3.1. Alloy properties

The composition, phase distribution, PCT characteristics, electrochemical properties, and magnetic susceptibility properties of